ELSEVIER

Journal of Alloys and Compounds 246 (1997) 248–255

Journal of ALLOYS AND COMPOUNDS

Effect of pressure on structural properties of intermetallic LnM lanthanide compounds

V.F. Degtyareva[a], F. Porsch[b], S.S. Khasanov[a], V.Sh. Shekhtman[a], W.B. Holzapfel[b]

[a]Institute of Solid State Physics, Academy of Science, Chernogolovka, Moscow District 142432, Russia
[b]FB 6 Physik, Universität-GH-Paderborn, 33095 Paderborn, Germany

Abstract

Energy dispersive powder X-ray diffraction measurements with diamond anvil high pressure cells at ambient temperature and pressure up to 50 GPa on the LnM compounds GdCu, LaAg, NdAg, NdZn, CeZn and LaZn show systematically high pressure phase transformations from the cP2 (CsCl-type) structure to lower symmetry phases, however, with only minor effects from valence instabilities.

Keywords: Lanthanide compounds; Structural properties; Pressure

1. Introduction

While most of the intermetallic LnM compounds of lanthanide metals Ln with either main group or transition metals M occur at ambient conditions in the cubic CsCl-type structure [1–3], henceforth denoted cP2 according to the recommended Pearson nomenclature [4], some of these compounds also show more complex structures like oP8 (FeB-type) or oC8 (CrB-type) [1–3]. In some cases, magnetic or martensitic (distortive or displacive) transitions were also observed at low temperatures [5,6] with strong effects of alloying [7,8], but few of these compounds have been studied up to now under pressure, for instance LnAg compounds with Ln = La, Ce, Pr, Nd up to 3.6 GPa [9–11] or CeZn up to 10 GPa [12,13].

Especially with respect to CeZn, the question arose as to whether the Kondo behaviour [12,13] or, in other words, contributions from valence instability or 4f hybridisation with the conduction electrons would cause some special effects in the Ce compounds and possibly in Nd compounds at higher pressure in comparison with La or Gd compounds, with only minor contributions from 4f hybridisation. In the case of Gd, stable magnetic moments would be expected even in extended ranges of pressures, for example up to 50 GPa.

2. Experimental details

Polycrystalline samples of LnM compounds were prepared from Ln metals of 99.9% and M metals of 99.999% purity by arc-melting in a pure argon atmosphere. X-ray powder diffraction and X-ray fluorescence analysis confirmed the known cubic structure at ambient conditions. High pressures were generated with a diamond anvil cell [14] using mineral oil as pressure transmitting medium. Ruby pressure sensors [15] together with the non-linear ruby scale [16] were applied for pressure measurements. Energy dispersive X-ray diffraction (EDXD) was performed with a conventional tungsten tube X-ray generator in the laboratory, and with synchrotron radiation at HASYLAB/DESY, as described in detail earlier [17,18]. The data collection time was typically 8 h and 15 min respectively. Diffraction spectra of most of the compounds were obtained on increasing the pressure up to 50 GPa, and subsequently also on decreasing the pressure to ambient conditions to verify the reversibility of all the observed transformations and to control possible sample decomposition or contamination. About 30 spectra were measured for each sample, and at least three samples of each compound were investigated. The energy dispersive spectra were analyzed and indexed with the use of specially developed software [19].

3. Results

All the samples of the present study showed very clear signs of more or less reversible phase transitions to lower symmetry structures even at moderate pressures of 2 to 12 GPa, in most cases with strong effects of hysteresis and texture, which complicated the analysis of the spectra.

0925-8388/97/$17.00
PII S0925-8388(96)02456-5

While the gross spectral features of all these compounds show some similarity at higher pressure, some individual features were observed at intermediate pressures and deserve more detailed discussion.

3.1. GdCu

At ambient conditions the present polycrystalline samples of GdCu exhibit diffraction patterns (Fig. 1) typical for the cP2 structure with $a_0 = 351(1)$ pm, in agreement with previous data [1]. On increasing the pressure above 12.8 GPa or decreasing it down to about 12 GPa the spectra show a pronounced splitting (Fig. 1) which is indexed by the present software [19] according to an orthorhombic unit cell oP4 as shown in Table 1.

Fig. 2 illustrates the corresponding variations in the lattice parameters a, b and c, in the axial ratios c/a and b/a, and in the volume V per formula unit with the axis assigned according to a pseudo αU-type structure oS4; however, due to the two different kinds of atom in this compound, the occurrence of weak superlattice reflections like 011, 100 and 112 in Table 1 points to an ordered structure oP4 (AuCd-type), bearing in mind that the αU-type structure occurs by a shuffling of layers plus distortion of the unit cell (Burgers mechanism) as an intermediate orthorhombic structure between the body-centred cubic cI2 and the hexagonal close-packed hP2 structures of the elements. In fact, if the axial ratios approach the special values $\sqrt{3} = 1.732$ and $\sqrt{8/3} = 1.633$, one obtains a hP2 structure.

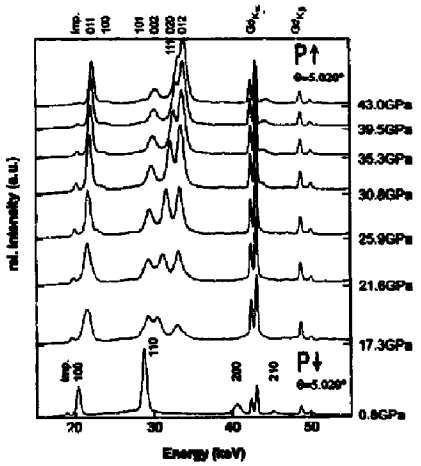

Fig. 1. Energy dispersive X-ray diffraction spectra of GdCu under pressure. The spectrum at 0.8 GPa was obtained on decompression. One weak impurity line also present after decompression in the cP2 phase is denoted by "Imp.".

Table 1
Observed and calculated interplanar spacings for the GdCu sample at 25.9 GPa according to Fig. 1. The values for $d_{obs} = 619.92$ keV pm/$(E_{obs} \sin\theta)$ are derived from least-squares fits of Gaussian lines to the spectra with the given value for θ. The values for d_{calc} are evaluated for the oP4 structure with the best fit values for $a = 304.2$ pm, $b = 448.1$ pm, and $c = 481.4$ pm

d_{obs} (pm)	d_{calc} (pm)	hkl
327.0	328.0	011
312.3	304.2	100
257.5	257.2	101
241.0	240.7	002
223.9	224.1	020
	223.1	111
206.3	203.1	021
174.5	174.0	112
164.2	164.0	022
150.8	152.1	200
	151.1	013
144.2	144.4	122
	144.0	210
127.2	126.9	032
121.9	121.8	221
119.2	119.9	123
116.5	116.2	014
112.5	112.0	040

This trend was also observed in the variation of the diffracted intensities. However, since it is well known from all the spectra of the other samples that the intensities of the present spectra are commonly affected by texture, much caution is required even in a qualitative discussion of the observed intensities. Furthermore, it must be pointed out that some weak additional peaks are also observed in all the spectra, as shown for instance in Fig. 1 for the well-known cP2 phases on decreasing the pressure to 0.8 GPa. These features are most reasonably explained by small amounts of oxide or other contaminants present in the sample space.

3.2. LaAg

The experimental data for LaAg in Fig. 3 look, at first glance, somewhat confusing. The weak shoulder at 25.4 keV of the first peak in the 1.2 GPa spectrum at 24.8 keV must be attributed to the K_β line of Ag, which is then resolved at higher pressures. This same 110 peak of the 1.3 GPa spectrum still shows the expected linewidth for the initial cP2 structure, however, the intensities of the corresponding cubic 111 peak at 30.4 keV and of the 200 peak at 35.4 keV are unusually weak due to effects of texture or grain size in these tiny samples. Effects of line splitting are visible on increasing the pressure at first around 3.4 GPa. If one uses the same oP4 indexing as for GdCu for the few well-resolved lines of these LaAg samples, one obtains the lattice parameters given in Fig. 4

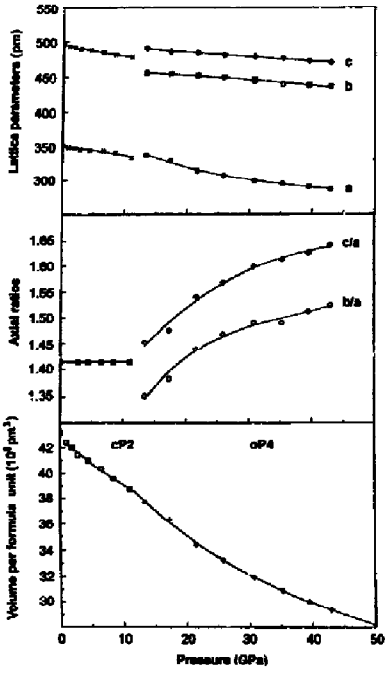

Fig. 2. Lattice parameters, axial ratios c/a and b/a, and volume per formula unit for the oP4 cell of GdCu under pressure. (The typical precision of the data is represented by the size of the symbols.)

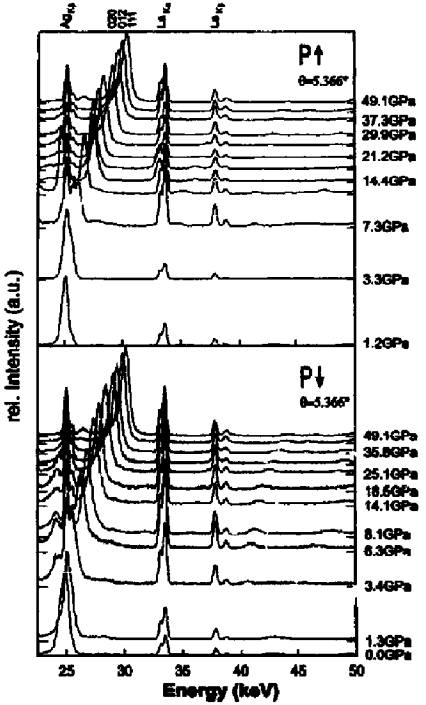

Fig. 3. Energy dispersive X-ray diffraction spectra of LaAg for increasing pressure (P↑) and decreasing pressure (P↓).

together with the axial ratios and the volume per formula unit. In this case both axial ratios appear to increase directly at the phase transition, and c/a seems to exceed the special value of $\sqrt{3} = 1.732$ at pressures between 20 and 25 GPa, when the structure is approaching a hP2-like structure.

On decreasing the pressure complete reversibility is observed, but with significant hysteresis not only in the lattice parameters but also in the volume data (Fig. 4). This kind of hysteresis is not completely unexpected for compacted polycrystalline samples and martensitic phase transitions. However, due to effects of texture, especially in the region of special values of c/a or b/a, where some of the lines are only poorly resolved, it cannot be excluded with complete certainty that these effects are only artefacts of the data analysis. Therefore, further experimental studies are required to obtain more definite results for these special regions. Nevertheless, the general trend in the volume decrease corresponds to the variation expected already from the well-known data [16,20] for the two constituent elements.

3.3. NdAg

The general trend in the data for NdAg is similar to the observations for LaAg, however, with many more lines observed in the spectra at higher pressure to support the structural assignment as shown in Table 2, which corresponds to the pattern for 47.3 GPa given in Fig. 5(b). Owing to the overlap of some of the diffraction lines with the fluorescence lines, either of Ag or Nd around 25 keV and 38 keV respectively, different diffraction angles were used for different runs to observe all the diffraction lines more clearly, as illustrated in Fig. 5(a) and Fig. 5(b). While Fig. 5(a) shows very clearly the first occurrence of additional diffraction lines of a low symmetry phase on increasing the pressure to 5.0 GPa, in Fig. 5(b) the 101, 012+020 and 111 triplet at 47.3 GPa as well as the 121, 113, 131 and 123 lines at higher energies are much more clearly resolved. Special effects of texture seem to suppress almost completely the 101 line at 43.4 GPa in Fig. 5(a). The occurrence of special relations for the orthorhombic axial ratios corresponding to the much simpler

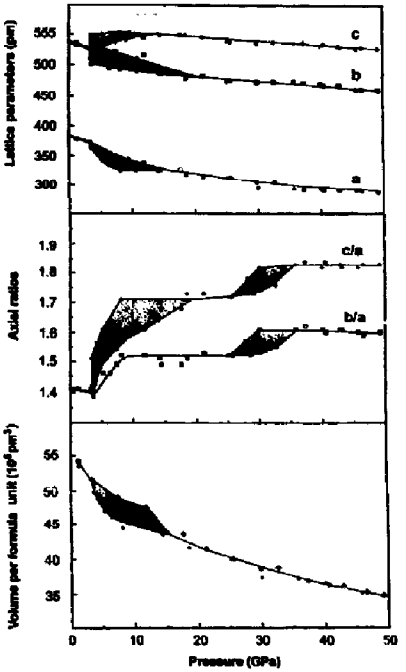

Fig. 4. Lattice parameters, axial ratios c/a and b/a, and volume per formula unit for the oP4 cell of LaAg: open symbols for increasing pressure, filled symbols for decreasing pressure, shadowed areas illustrate hysteresis.

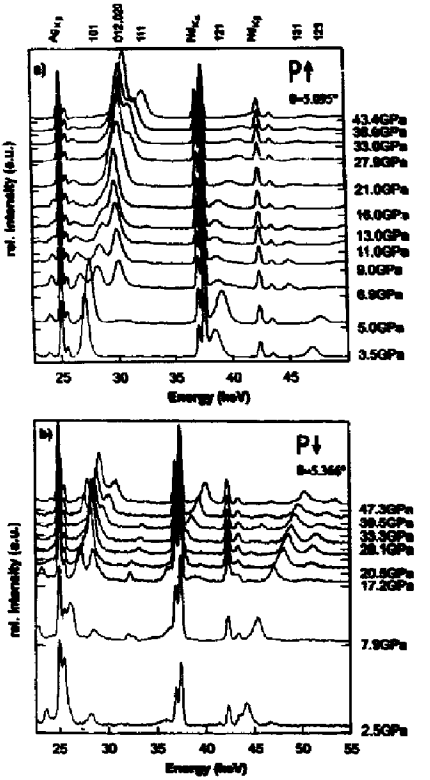

Fig. 5. Energy dispersive X-ray diffraction spectra of the NdAg compound under pressure for increasing (P↑) and decreasing (P↓) pressure using different diffraction angles for the two series (a) and (b).

pattern of an almost hexagonal structure is clearly visible in the spectra around 20 GPa in both spectral series.

With the same oP4 indexing scheme used for GdCu and LaAg, one obtains the lattice parameter values illustrated in Fig. 6. Obviously, the orthorhombic distortions seem to show rather large differences for the two different runs on the same sample material, possibly due to the low values of the principle elastic coefficients C_{ii} and the presence of local deviatoric stresses coupled to texture with some hysteresis most clearly observed around 28 GPa in the variation of the axial ratios. In fact, the axial ratio $c/a = \sqrt{3} = 1.732$ corresponds to the hexagonal lattice, and it appears reasonable to assume that special contacts of the Fermi surface with boundaries of the Brillouin zone in the corresponding hexagonal lattice result in a special lowering of the structural energy, which could possibly explain the anomalous variation of the c/a ratio when this special value tends to be surmounted on increasing the pressure. However, it is not completely clear whether this apparent hysteresis could not also be caused spuriously by texture

Table 2
Observed and calculated interplanar spacings for the NdAg sample at 47.3 GPa according to Fig. 5(b). The values for $d_{obs} = 619.92$ keV pm/$(E_{obs} \sin\theta)$ are derived from least-squares fits of Gaussian lines to the spectra with the given value for θ. The values for d_{calc} are evaluated for the oP4 structure with the best fit values for $a = 277.8$ pm, $b = 453.4$ pm, and $c = 526.8$ pm

d_{obs} (pm)	d_{calc} (pm)	hkl
244.0	245.7	101
227.7	227.8	012
227.0	226.7	020
216.5	216.0	111
165.6	166.6	121
141.4	141.1	113
131.7	131.7	004
	131.1	032
129.0	128.7	131
124.0	124.2	123

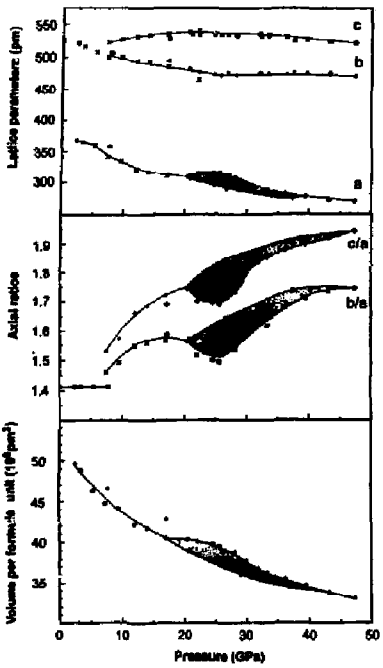

Fig. 6. Lattice parameters, axial ratios c/a and b/a, and volume per formula unit for the oP4 cell of NdAg: open symbols for increasing pressure, full symbols for decreasing pressure, shadowed areas illustrate apparent hysteresis.

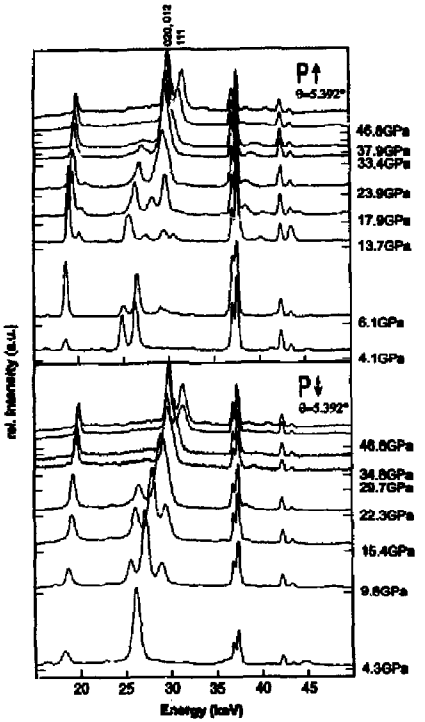

Fig. 7. Energy dispersive X-ray diffraction spectra of NdZn for increasing pressure (P↑) and decreasing pressure (P↓).

and unusual intensity relations, resulting in larger ambiguities in the evaluation of the lattice parameters in the region of strongly overlapping lines near this special value of $c/a = \sqrt{3}$.

3.4. NdZn

If one takes into account the always observed effects of texture on the intensities of the present diffraction data, the spectra for NdZn presented in Fig. 7 are very similar to the spectra for NdAg given in Fig. 5, and the same phenomenon of rather large deviations in the orthorhombic splittings on increasing with respect to decreasing pressure is also observed for the lattice parameters and axial ratios, presented in Fig. 8 together with the corresponding values for the volume per formula unit. By comparison of the data for increasing and decreasing pressure, the cP2–oP4 transition can be located rather precisely at 4.2 GPa (Fig. 8). Assignments of the diffraction lines for one typical spectrum of this new oP4 phase are given in Table 3.

3.5. CeZn

Owing to the problems with fluorescence lines, diffraction data for CeZn were recorded for different diffraction angles as shown in Fig. 9, which also includes one set of data for decreasing pressure to illustrate more clearly the complex situation at intermediate pressures, between 4 and 16 GPa, and, furthermore, the complete reversibility to the cP2 structure at pressures below 2 GPa. In addition, the second set of data (Fig. 9(c)) illustrates the strong effects of texture, which suppress almost completely one of the strongest lines of the first set (Fig. 9(a) and Fig. 9(b)) around 26 keV at the highest pressures as well as the higher energy lines around 37 and 45 keV respectively.

With these problems of texture in mind, the spectra above 16 GPa are indexed most readily to the oP4 structure with reasonable values for the lattice parameters, axial ratios, and volume per formula unit as shown in Table 4. With this indexing one can trace some of the lines down to about 11 GPa, with the results also illustrated in Fig. 10.

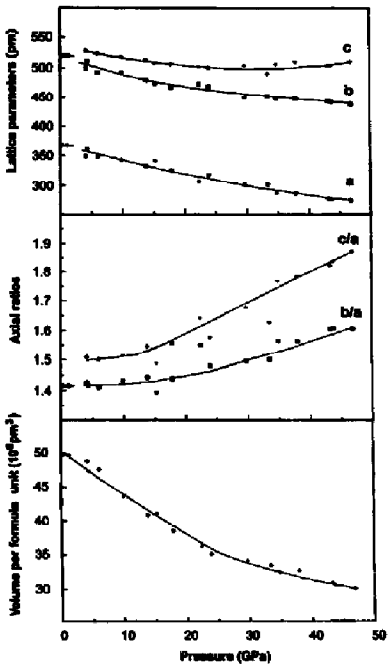

Fig. 8. Lattice parameters, axial ratios c/a and b/a, and volume per formula unit for the cP4 cell of NdZn: open symbols for increasing pressure, full symbols for decreasing pressure.

However, this procedure does not explain all the lines observed in the intermediate region, giving some hints at phase mixture and possibly complicated structures.

It can be noted that two high pressure structural studies had been performed before on CeZn, one single crystal neutron diffraction study [12] at temperatures below 60 K and pressures up to 1.2 GPa and one angular dispersive powder X-ray diffraction study [13] up to 10 GPa, which confirmed to some extent the first observation [12] of a cubic to rhombohedral transition observed at low temperatures, between 30 and 60 K, with transition pressures increasing from 1.1 to 1.2 GPa in this limited range of temperatures, in reasonable agreement with the later [13] location of this transition at room temperature and 2.6 GPa. However, the observation of many more diffraction lines in the present study in comparison with the previous measurements [13] leads to the suspicion that the situation is more complicated in this intermediate region, with the possible occurrence of one metastable (rhombohedral) phase according to a distortive transition and a second (more stable?) phase formed under stronger kinetic hindrance, similar to the situation in elemental Ce [21,22].

Table 3
Observed and calculated interplanar spacings for the NdZn sample at 13.7 GPa according to Fig. 7(a). The values for $d_{obs} = 619.92$ keV pm/$(E_{obs} \sin\theta)$ are derived from least-squares fits of Gaussian lines to the spectra with the given value for θ. The values for d_{calc} are evaluated for the oP4 structure with the best fit values for $a = 336.1$ pm, $b = 477.2$ pm, and $c = 514.2$ pm

d_{obs} (pm)	d_{calc} (pm)	hkl
350.2	349.8	011
331.6	336.1	100
281.8	281.4	101
259.0	257.1	002
242.1	242.4	111
	238.6	020
225.0	226.3	012
216.8	216.4	021
164.6	161.3	013
151.8	152.7	103
	152.0	031
135.6	135.3	032
	134.9	211
129.1	128.6	123
	128.6	004
123.4	124.1	014
114.5	113.2	024
110.4	110.2	133
	109.8	141
106.0	106.7	311
	105.4	232

3.6. LaZn

Some first data for LaZn under pressures up to 46 GPa are given in Fig. 11 to illustrate, at least qualitatively, that the structural sequence seems to be similar to that of CeZn; however with the complex 'intermediate' region extending down to ambient pressure, as indicated by the complex pattern after complete release of the pressure, and up into the region around 30 GPa, where the same kind of simple pattern as in CeZn around 16 GPa seems to occur.

4. Discussion

In contrast to what might have been expected, all the LnM compounds studied so far transform from the ambient pressure cP2 structure to lower symmetry phases at rather moderate pressures, with no clear distinction between compounds of the electronically 'stable' lanthanides, like La and Gd, and the 'irregular' lanthanides, like Ce and Nd, which are well known to exhibit, in their elemental form, valence transitions, intermediate valencies, or at least strong f–d hybridisation phenomena under high pressure [23]. Even without final results for the intermediate pressure ranges in the case of LaAg, CeZn and LaZn, a general trend of structural phase transitions to one common prototype structure at higher pressures is noticed with reasonable results for an oP4 indexing and with more or

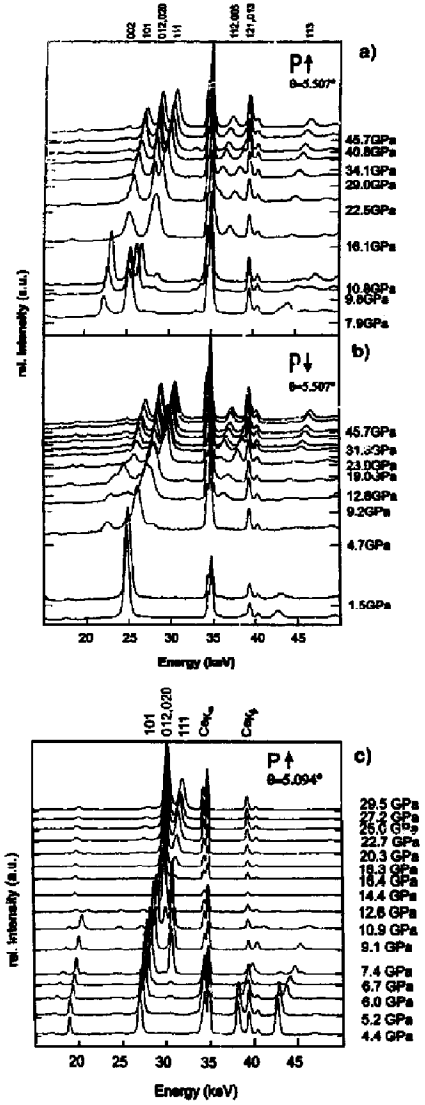

Fig. 9. Energy dispersive X-ray diffraction spectra of the CeZn compound under pressure. Two series with different diffraction angles are illustrated in (a,b) and (c).

Table 4
Observed and calculated interplanar spacings for the CeZn sample at 45.7 GPa according to Fig. 7(a). The values for $d_{obs} = 619.92$ keV pm/$(E_{obs} \sin\theta)$ are derived from least-squares fits of Gaussian lines to the spectra with the given value for θ. The values for d_{calc} are evaluated for the oP4 structure with the best fit values for $a = 270.4$ pm, $b = 445.0$ pm, and $c = 522.9$ pm

d_{obs} (pm)	d_{calc} (pm)	hkl
260.8	261.5	002
239.3	240.2	011
224.2	225.4	012
	222.5	020
211.7	211.3	111
186.4	187.9	102
173.5	173.1	112
163.0	163.2	121
138.9	139.1	113
130.9	130.9	201
	130.7	004
122.6	122.4	123
116.4	116.4	132
	115.9	212
111.3	111.2	040

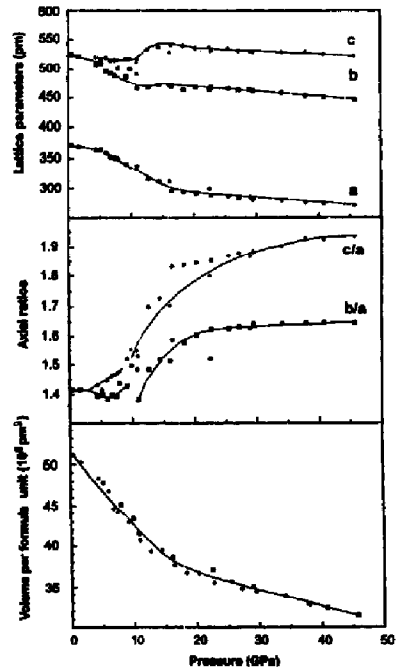

Fig. 10. Lattice parameters, axial ratios c/a and b/a, and volume per formula unit for the oP4 cell of CeZn: open symbols for increasing pressure, full symbols for decreasing pressure.

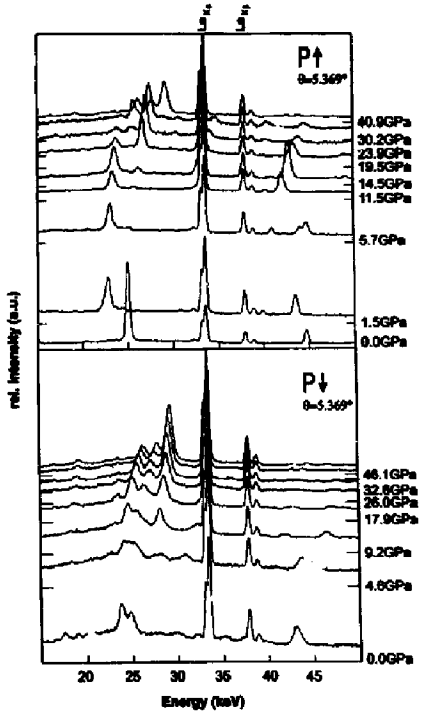

Fig. 11. Energy dispersive X-ray diffraction spectra of LaZn for increasing pressure (P↑) and decreasing pressure (P↓).

less continuous increases in the orthorhombic distortions up to the highest pressures.

Besides these major features, many details of the structural assignment for possible intermediate phases, some unusual hysteresis, and strong tendencies to exhibit textures need further investigation.

Acknowledgments

Technical support by Jens Otto at the EDXD station in HASYLAB at DESY, Hamburg, as well as financial support for the German side by the Deutsche Forschungsgemeinschaft (DFG) and for cooperation with the Russian side by NATO under Grant No. HTECH.CRG 930756 and by the International Science Foundation under Grant No. NKR 000 are gratefully acknowledged.

References

[1] W.B. Pearson, *Handbook of lattice spacings and structures of metals and alloys*, Vol. 2, Pergamon Press, New York, 1967, p. 1446.
[2] K.N.R. Taylor, *Adv. Phys.*, *20* (1971) 551.
[3] P. Villars and L.D. Calvert, *Pearson's Handbook of Crystallographic Data for Intermetallic Phases*, Vol. 1–3, American Society for Metals, Metals Park, OH, 1986, p. 3258.
[4] G.J. Leigh (ed.), *Nomenclature of Inorganic Chemistry*, Blackwell Scientific, Oxford, 1990.
[5] H. Balster, H. Ihring, A. Kockel and S. Methfessel, *Z. Phys. B*, *21* (1975) 241.
[6] D. Schmitt, P. Morin and J. Pierre, *J. Magn. Magn. Mater.*, *8* (1978) 249.
[7] J. Mucic, M. Müllner, H. Jex, W. Assmus and R. Takke, *Z. Phys. B*, *37* (1980) 39.
[8] H. Ihrig and S. Methfessel, *Z. Phys. B*, *24* (1976) 385.
[9] H. Ihrig, D.T. Vigren, J. Kübler and S. Methfessel, *Phys. Rev. B*, *8* (1973) 4525.
[10] J.S. Schilling, S. Methfessel and R.N. Shelton, *Solid State Commun.*, *24* (1977) 659.
[11] M. Kurisu, *J. Phys. Soc. Jpn.*, *56* (1987) 4064.
[12] T. Shigeoka, Y. Uwatoko and H. Fujii, *Phys. Rev. B*, *42* (1990) 8394.
[13] Y. Uwatoko, K. Suenaga and G. Oomi, *J. Magn. Magn. Mater.*, *104* (1992) 645.
[14] K. Syassen and W.B. Holzapfel, *Europhys. Conf. Abstr.*, *1A* (1975) 75.
[15] R.A. Forman, G.I. Piermarini, J.D. Barnett and S. Block, *Science*, *176* (1972) 284.
[16] H.K. Mao, P.M. Bell, J.W. Shaner and D.J. Steinberg, *J. Appl. Phys.*, *49* (1978) 3276.
[17] W.B. Holzapfel and W. May, in S. Akimoto and M.H. Manghnani (eds.), *High Pressure Research in Geophysics*, Advances in Earth and Planetary Sciences, Vol. 12, Center for Academic Publishing, Tokyo, 1982, 73.
[18] W.A. Grosshans, E.-F. Düsing and W.B. Holzapfel, *High Temp.-High Press.*, *16* (1984) 539.
[19] EDXPowd, XPowder, copyright F. Porsch, Paderborn, 1993.
[20] W.A. Grosshans and W.B. Holzapfel, *Phys. Rev. B*, *45* (1992) 5171.
[21] J. Staun Olsen, L. Gerward, U. Benedict and J.-P. Itie, *Physica B*, *133* (1985) 129.
[22] Y. Zhao and W.B. Holzapfel, *J. Alloys Comp.* (1996) this issue.
[23] W.B. Holzapfel, *J. Alloys Comp.*, *223* (1995) 170.